

Diffusion of 18 elements implanted into thermally grown SiO₂

H. G. Francois-Saint-Cyr

School of Optics, University of Central Florida, Orlando, Florida 32816

F. A. Stevie

Analytical Instrumentation Facility, North Carolina State University, Raleigh, North Carolina 27695

J. M. McKinley

Agere Systems, 9333 South John Young Parkway, Orlando, Florida 32819

K. Elshot

School of Optics, University of Central Florida, Orlando, Florida 32816

L. Chow^{a)}

Department of Physics, University of Central Florida, Orlando, Florida 32816

K. A. Richardson

School of Optics, University of Central Florida, Orlando, Florida 32816

(Received 13 June 2003; accepted 18 September 2003)

Diffusion data are presented for 18 elements implanted in SiO₂ layers thermally grown on silicon and annealed at temperatures ranging from 300 to 1000 °C. Most species studied, (e.g., Be, B, Al, Sc, Ti, V, Zn, Ga, and Mo), showed negligible diffusion over the examined temperature range. In general, this study has shown that the diffusivity of dopants or impurities in SiO₂ is significantly smaller than that in silicon. However we also observed that several elements (e.g., Rb and In) have a higher diffusivity in SiO₂ than in Si. Because Ga and In are both used as sources for focused ion beam analyses, the lack of Ga diffusion and the movement of In in SiO₂ is of interest. © 2003 American Institute of Physics. [DOI: 10.1063/1.1624487]

I. INTRODUCTION

The study of diffusion of impurities in solids continues to be an area of significant interest. Knowledge of the manner in which different species diffuse in a material provides information that is required to determine the impurities that will be most likely to negatively impact the desired properties of the material. Decisions can then be made on the contaminants that need to be removed and those that can be tolerated in a matrix. The transport of an impurity in a material may not be the same even when compared with a matrix that would appear to be similar. Addition of other impurities to the matrix may retard or advance the ability of a species to diffuse. SiO₂ is an important insulating material with broad applications in the semiconductor and glass industries, and ion mobility in silicate structures can affect the physical properties of the glasses.

Diffusion of impurities in silicon has been studied extensively since the 1960s, primarily by the method of surface deposition followed by anneals.¹⁻³ Because of the technological importance of silicon, a large body of data exists on the diffusion of dopants and impurities in silicon.⁴⁻⁶

Diffusion of impurities in SiO₂ was much less studied than Si.⁷ Ghozzo and Brown⁸ reviewed the diffusivities of doping elements such as B, Ga, P, As, and Sb. Besides a few summary papers,⁹⁻¹¹ most diffusion data of impurities in SiO₂ are scattered throughout the literature.¹²⁻²⁶ The net-

work structure of vitreous SiO₂ also suggests the importance of self diffusion of O₂ and Si in SiO₂. In the early 1980s, Brebec *et al.*²⁷ and Schaeffer²⁸ reported on the self diffusion of Si and O₂ in SiO₂. Pfeffer and Ohring²⁹ has shown the importance of oxygen exchange between SiO₂ network and H₂O molecule in the diffusion mechanism of H₂O diffusion in SiO₂ thin films. More recently, both *ab initio* calculation of oxygen self diffusion in α -quartz³⁰ and secondary ion mass spectrometry (SIMS) measurements of network oxygen in vitreous SiO₂³¹ have reconfirmed the earlier work.^{27,28}

Ion implantation presents a flexible approach to the study of diffusion. The depth of the peak implant concentration can be regulated by the implantation energy and the concentration by the implanted dose. The implant dose can be varied to provide a concentration range from ppm to a few atomic percent. All elements and isotopes can be implanted. Therefore, ion implantation can be used for diffusion studies of a surface layer, a sublayer, or the interface between layers. It is important to recognize that the implant dose can affect the diffusion, especially if the dose is sufficient to amorphize the matrix under investigation.³²

The results for nondopant elements implanted into silicon have not been as comprehensive as expected, and this realization helped initiate our recent work in this area.³³ From literature data, we anticipate that for most impurities diffusion in silica would take place at a lower rate than for silicon. Studies of implanted elements in silica have been limited and were done mostly at high doses (10¹⁵ atoms/cm² and higher) implanted at high energies with analyses made

^{a)} Author to whom correspondence should be addressed; electronic mail address: chow@ucf.edu

TABLE I. Implantation parameters.

Element	Energy (keV)	Dose (cm ⁻²)
⁹ Be	70	1.0×10 ¹⁴
¹¹ B	50	1.0×10 ¹⁵
¹⁹ F	50	5.0×10 ¹⁴
²⁷ Al	50	1.0×10 ¹⁴
³⁵ Cl	150	5.0×10 ¹⁴
⁴⁰ Ca	150	1.0×10 ¹⁴
⁴⁵ Sc	150	1.0×10 ¹⁴
⁴⁸ Ti	150	1.0×10 ¹⁴
⁵¹ V	150	1.0×10 ¹⁴
⁵⁵ Mn	150	1.1×10 ¹⁴
⁶⁴ Zn	180	3.3×10 ¹⁴
⁶⁹ Ga	180	8.0×10 ¹³
⁷⁹ Br	180	1.2×10 ¹⁴
⁸⁰ Se	180	1.9×10 ¹⁴
⁸⁵ Rb	180	7.5×10 ¹³
⁹⁸ Mo	180	8.9×10 ¹³
¹¹⁵ In	210	9.2×10 ¹³
¹²⁷ I	180	8.8×10 ¹³

using Rutherford backscattering spectrometry (RBS). For example, van Ommen has studied the diffusion behavior of implanted As, Ga, Tl, and Sb in silica using RBS.^{34–38}

The intent of the current study is to extend the study of diffusion in SiO₂, using ion implantation to introduce the impurity and SIMS for characterization of the implanted and annealed samples. The elements of interest are implanted at doses that keep the maximum concentration below 0.1 at. %. The consideration of amorphizing dose is less significant here because the silica layer is already amorphous. The ion implantation is made into a thermally grown silica layer on a silicon substrate. SIMS has the sensitivity and depth resolution required for this analysis, but mobility of species during analysis must be taken into account, especially for alkali elements.^{39,40} It has been noted that other species, such as N, can also move during analysis.⁴¹

II. EXPERIMENTAL PROCEDURE

The substrates used in this work were *p*-type (100) oriented Si wafer with a nominal resistivity of 10–20 Ω cm. The growth of oxide layer was carried out in a steam furnace. The elements shown in Table I were separately implanted into 0.49 μm thick thermally grown silica layers at approximately 10¹⁴ atoms/cm² using a variety of implanters. Dose accuracy was checked from analysis of identical samples implanted into silicon. The implants in silicon were checked against existing standards. The dose was specifically chosen to study the movement of a low concentration (about 0.1 at. % maximum) of a species in silica and to permit a good dynamic range of detection using SIMS. The implant energy was selected to locate each species within the silica layer, and ranged between 50 and 210 keV. The Be implant energy put the peak of the Be implant near the silica/silicon interface. However, the diffusion data obtained from the part of the implant that was in the silica still provides useful information.

Anneals were made at 300, 500, 700, 900, and 1000 °C in a Lindberg furnace. All anneals were for 30 min with a

constant flow of high purity argon gas (99.999%). The samples were placed in a quartz tube that was moved into the center of the furnace for heating, and pulled out to be cooled to room temperature, all within an argon environment.

The samples were analyzed using three SIMS instruments. Most samples with high positive secondary ion yields under oxygen bombardment were analyzed using a CAM-ECA IMS-3f magnetic sector analyzer with 10 keV O₂⁺ primary beam, impact energy of 5.5 keV, and effective impact angle of 42° from normal. A typical primary beam current was 120 nA rastered over a 250 μm by 250 μm area with secondary ions detected from a 60 μm diam circle at the center of the raster. Charge neutralization was accomplished with an oblique incidence electron gun, with an energy of approximately 5 keV, and impact energy of approximately 10 keV because of the additional effect of the positive 4.5 keV sample potential. Some samples were analyzed using a CAMECA IMS-6F with O₂⁺ primary beam and charge neutralization with normal incidence electron gun. Elements with high negative secondary ion yields under cesium bombardment were analyzed using a Physical Electronics ADEPT 1010 quadrupole analyzer with a 3 keV Cs⁺ primary beam at 60° from normal. For these analyses, the typical primary beam current was 100 nA rastered over a 200 μm by 200 μm area with negative secondary ions detected from the center 10% of the raster. Charge neutralization was made with an unrastered 5 μA 3 keV electron beam centered on the ion beam raster.

SIMS analysis of the as-implanted samples provided a check on distortions that might be present as a result of analysis using a charged beam because the as implanted profile should have a Gaussian shape.

III. RESULTS AND DISCUSSION

Figures 1–3 show SIMS depth profiles for nine elements as implanted and after anneal. As we can see from these figures, the peak of the distributions ranges between 0.1 and 0.25 μm from the film surface, except for ⁹Be, which has a peak concentration close to the SiO₂/Si interface. The major feature of the diffusion behavior of these nine elements is that even after a 1000 °C anneal for 30 min, these elements diffuse sparingly, if at all. In Fig. 1(a) we can see that the as-implanted sample showed that part of the implanted Be is present in the crystalline Si. Following annealing at 500 °C, these Be ions begin to move. Note that the Be implanted in the Si will not be accurately quantified by the implant in SiO₂ because of significantly lower secondary ion yield in the Si compared with the SiO₂. At 700 °C anneal, almost all Be ions have diffused out of the Si region just below the SiO₂ layer, but the Be in the SiO₂ layer shows essentially no movement in the temperature range of 300–1000 °C.

Even though the profiles in Figs. 1–3 show little diffusion, it was still possible to obtain an upper bound for diffusion coefficients for several elements using the following procedure. We assume that the impurity concentration will have a joint half Gaussian distribution.³⁵ Since the near-

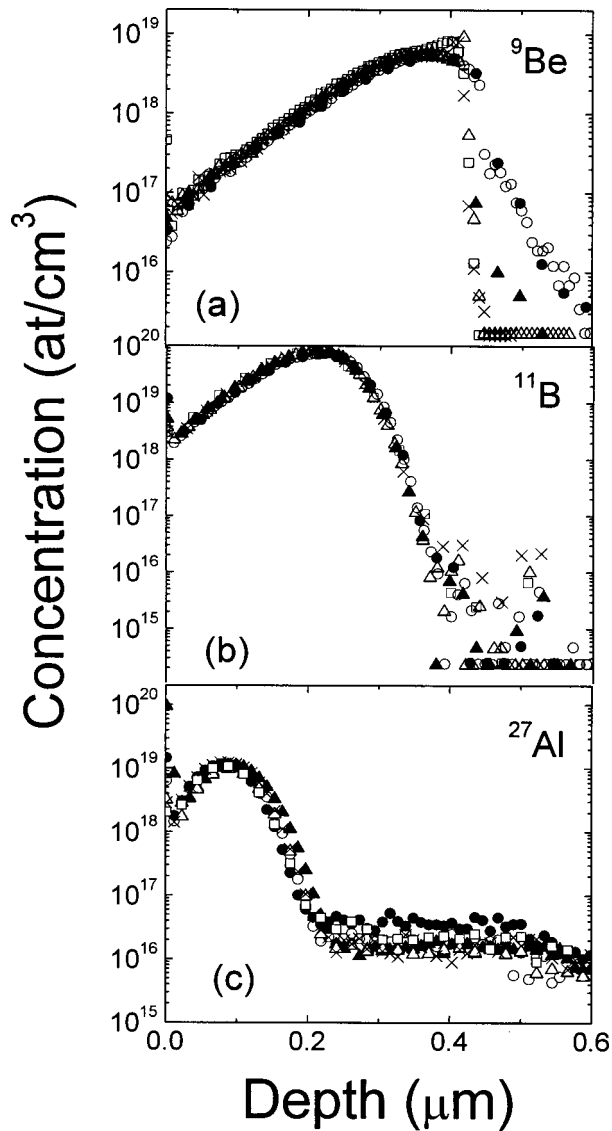


FIG. 1. SIMS depth profiles of: (a) ^9Be (70 keV, $1E14$ atoms/cm 2), (b) ^{11}B (50 keV, $1E15$ atoms/cm 2), (c) ^{27}Al (50 keV, $1E14$ atoms/cm 2): (●) as implanted, (○) 300 °C, (▲) 500 °C, (△) 700 °C, (×) 900 °C, (□) 1000 °C.

surface region will have more damage and defects that could affect diffusion and also impurity species near the surface, we will only use the concentration profile from the concentration peak to the SiO $_2$ /Si interface for the calculation of diffusion coefficients. This procedure has been previously documented.^{35,37} The concentration profile after anneal is given by

$$C(x) = C' \exp\left(\frac{-(x-x_m)^2}{2(\sigma^2 + 2Dt)}\right), \quad (1)$$

where x_m is the peak position and σ is the standard deviation of the as-implanted impurity distribution.

The diffusion coefficients of these elements were calculated from the semilog plots of the SIMS concentration profiles of the as-implanted and 1000 °C anneal data. In Fig. 1(a), because the concentration peak is too close to the SiO $_2$ /Si interface, we did not calculate the diffusion coefficient of Be in silica. Both B and Al implanted in SiO $_2$ have

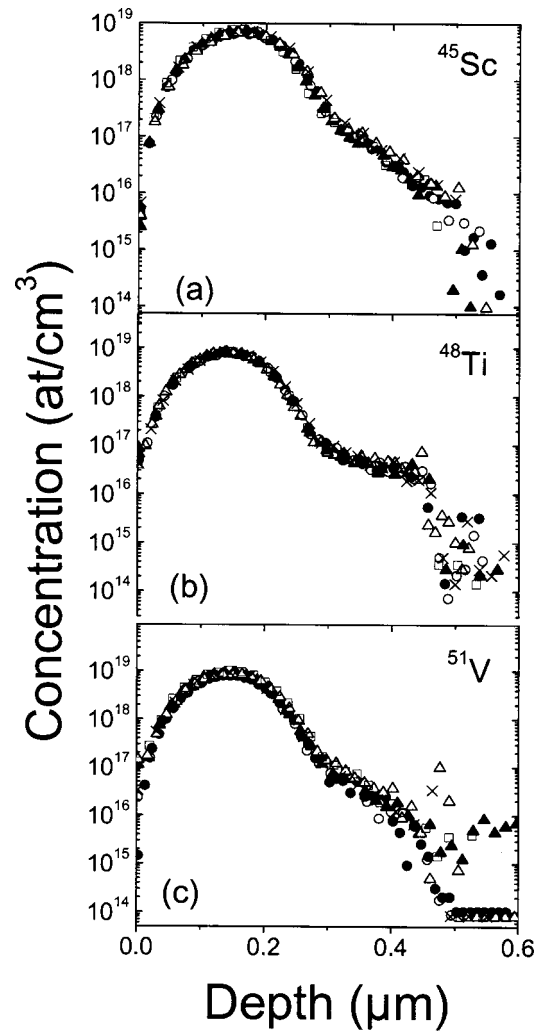


FIG. 2. SIMS depth profiles of: (a) ^{45}Sc (150 keV, $1E14$ atoms/cm 2), (b) ^{48}Ti (150 keV, $1E14$ atoms/cm 2), (c) ^{51}V (150 keV, $1E14$ atoms/cm 2): (●) as implanted, (○) 300 °C, (▲) 500 °C, (△) 700 °C, (×) 900 °C, (□) 1000 °C.

been studied before.^{42,43} For B (1000 °C) and Al (1200 °C) in SiO $_2$, the diffusion coefficients of 4.4×10^{-18} and 1.65×10^{-16} cm 2 /s, respectively, have been reported. Our data from Fig. 1(b) yield a diffusion coefficient of $6.0 \pm 1.0 \times 10^{-18}$ cm 2 /s for B, which is in good agreement with previously published data mentioned above. Figure 1(c) yields a diffusion coefficient of $< 5 \times 10^{-18}$ cm 2 /s for Al in SiO $_2$ at 500 °C. This value should be compared with 1.65×10^{-16} cm 2 /s at 1200 °C obtained by La Ferla *et al.*⁴³

In Figs. 2(a), 2(b), and 2(c) the diffusion behavior of Sc, Ti, and V implanted into the SiO $_2$ layer are shown. Here we notice that near the end of the implantation range, these elements showed higher concentration than expected from the normal detection limit. Even though mass interferences, such as $^{29}\text{Si}^{16}\text{O}$ with ^{45}Sc , can be resolved, no significant interference should exist for ^{51}V . We have used only the data that have an impurity concentration of $\geq 10^{17}$ atoms/cm 3 for our calculations. We obtained diffusion coefficients of $< 1.1(0.3) \times 10^{-18}$, $< 6 \times 10^{-19}$, and $< 1.8(0.2) \times 10^{-17}$ cm 2 /s for Sc, Ti, and V respectively. The lack of Ti diffusion in SiO $_2$ should be of interest for LiNbO $_3$ -SiO $_2$

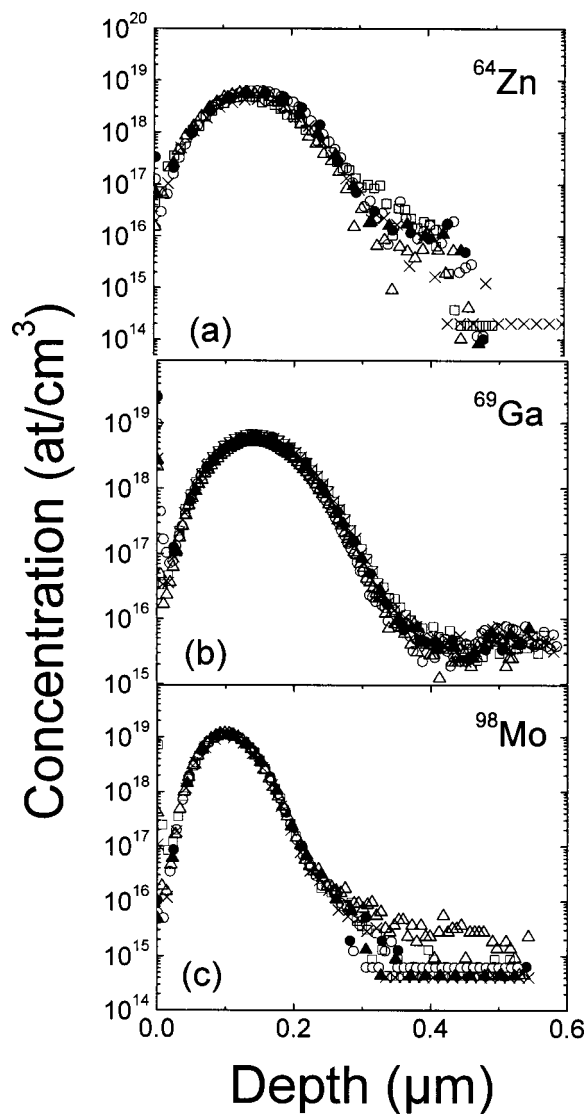


FIG. 3. SIMS depth profiles of: (a) ^{64}Zn (180 keV, $3.3E14$ atoms/cm 2), (b) ^{69}Ga (180 keV, $8E13$ atoms/cm 2), (c) ^{98}Mo (180 keV, $8.9E13$ atoms/cm 2): (●) as implanted, (○) 300 °C, (▲) 500 °C, (△) 700 °C, (×) 900 °C, (□) 1000 °C.

structures where Ti diffusion is used to change index of refraction for lightwave technology devices.

In Figs. 3(a), 3(b), and 3(c), SIMS depth profiles of Zn, Ga, and Mo implanted in SiO $_2$ are shown. Here again, the implanted species do not diffuse significantly when annealed at 300–1000 °C. Using the procedure described above, we obtained diffusion coefficients of $<6 \times 10^{-18}$ and $<8 \times 10^{-19}$ cm 2 /s for Ga and Mo, respectively, at 1000 °C. The diffusion behavior of Ga in silica has been studied before.³⁵ Van Ommen demonstrated that at 10^{15} Ga/cm 2 dosage, after annealing in N $_2$ ambient for 30 min at 1000 °C, the implanted Ga is immobile. The SIMS data for Zn implanted into silica showed some diffusion at low temperature anneals, but at higher temperatures such as 1000 °C, the Zn profile actually became narrower than that of the as-implanted sample. This narrowing of the concentration profile is believed to be due to the formation of impurity clus-

TABLE II. Diffusion coefficient of several elements in SiO $_2$.

Element	D (@ 1000 °C) (cm 2 /s) (from literatures data)	D (@ 1000 °C) (cm 2 /s) (present work)
B	4.4×10^{-18a}	$<6 \times 10^{-18}$
Al	1.65×10^{-16b}	$<5 \times 10^{-18c}$
Ca	...	$3.5 \pm 0.2 \times 10^{-16}$
Sc	...	$<1.1 \times 10^{-18}$
Ti	...	$<6 \times 10^{-19}$
V	...	$<1.8 \times 10^{-17}$
Mn	...	$8.8 \pm 0.1 \times 10^{-17}$
Ga	Immobile ^d	$<6.0 \times 10^{-18}$
Mo	...	$<8 \times 10^{-19}$
Si	9.8×10^{-19e} 1.3×10^{-18f}	
O	2.2×10^{-16g}	

^aSee Ref. 42.

^bAt 1200 °C, see Ref. 43.

^cAt 500 °C.

^dSee Ref. 35.

^eAt 1200 °C, see Ref. 27.

^fAt 1200 °C, see Ref. 46.

^gAt 1200 °C, see Ref. 47.

ters. This type of impurity clustering behavior has been observed previously in our laboratory.⁴⁴

In Table II, the diffusion coefficients are presented for seven out of the nine elements shown in Figs. 1–3. In addition, we also obtained values of diffusion coefficients for Ca and Mn in SiO $_2$ discussed below. We can see that the diffusion coefficients varied from 10^{-16} to 10^{-19} cm 2 /s at 1000 °C. For most elements that do not move appreciably, we only obtain an upper bound for the diffusion coefficients. In general, our results indicate that these elements have significantly less diffusion in silica than for the corresponding implants in silicon.

In Figs. 4(a) and 4(b), we showed that both Ca and Mn have a measurable diffusion coefficient in the 900–1000 °C temperature range. In Fig. 4(a), Ca starts to show movement during the 900 °C anneal. At 1000 °C, from the depth profile we calculated a diffusivity of $3.5 \pm 0.1 \times 10^{-16}$ cm 2 /s.

In Fig. 4(b), Mn did not move until the 1000 °C anneal. We again use procedures described in Ref. 16 and determine the diffusion coefficient of Mn in SiO $_2$ at 1000 °C to be $9 \pm 0.2 \times 10^{-17}$ cm 2 /s. In Fig. 4(c), the Se profiles show stability up to 700 °C anneal. After 900 °C anneal, the tail end of the profile starts to diffuse deeper into the oxide. After 1000 °C anneal, the profile distribution of Se impurity is similar to the Ca or Mn after 1000 °C anneal. Because of the scatter in the SIMS data we did not obtain a diffusion coefficient for Se.

Next we will examine the more mobile species in our current study. For Rb, after a 300 °C anneal, the depth profile changes very little compared to the as-implanted sample. But with a 500 °C anneal, it can be seen that Rb starts to diffuse. The maximum to minimum concentration ratio of Rb inside the SiO $_2$ layer has decreased by a factor of 1000 from the 300 °C anneal to the 700 °C anneal. After a 1000 °C anneal, the Rb concentration becomes constant inside the SiO $_2$ layer. We noted that the Rb background has increased going from SiO $_2$ to silicon. This may be due to a mass interference with

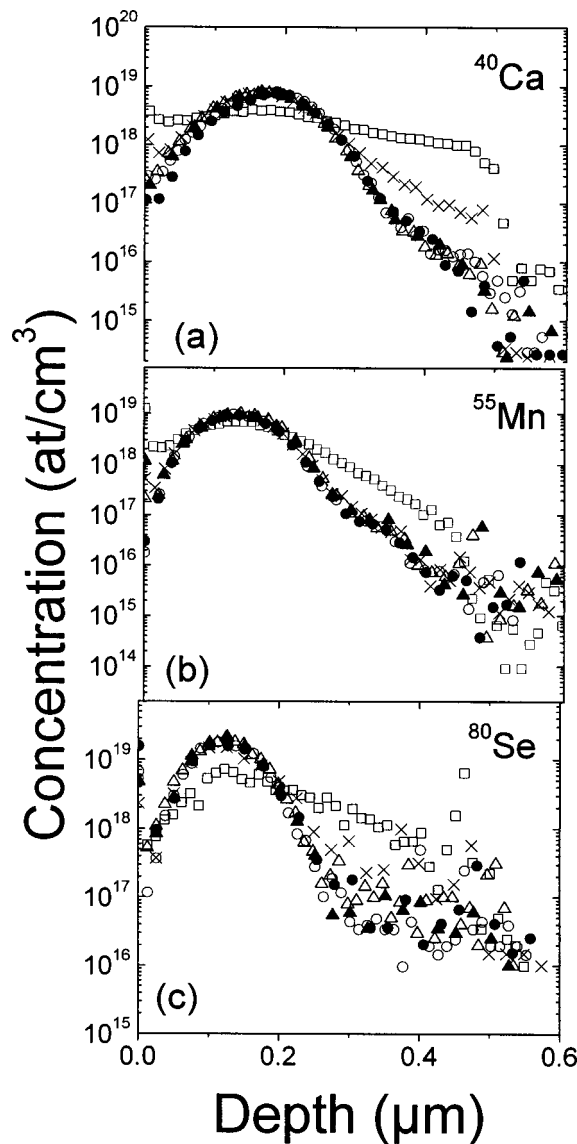


FIG. 4. SIMS depth profiles of: (a) ^{40}Ca (150 keV, $1E14$ atoms/cm 2), (b) ^{55}Mn (150 keV, $1.1E14$ atoms/cm 2), (c) ^{79}Se (180 keV, $1.9E14$ atoms/cm 2): (●) as implanted, (○) 300 °C, (▲) 500 °C, (△) 700 °C, (×) 900 °C, (□) 1000 °C.

$^{28}\text{Si}_2$ ^{29}Si that is more significant in Si than in SiO $_2$. It is noted that while most elements have a smaller diffusion coefficient in SiO $_2$ than in silicon, Rb is an exception. The diffusion coefficient of Rb in SiO $_2$ seems to be much larger than that in Si.¹⁴ Presumably this may have to do with the strong chemical reaction between Rb and oxygen and the fact that Rb seems to form clusters in Si.

In Fig. 5(b), depth profiles of In implanted in SiO $_2$ are shown. Up to 700 °C, there is not much movement of the In. Following a 900 °C anneal, the In impurity has clearly diffused toward the SiO $_2$ /Si interface. After a 1000 °C anneal, the concentration of In impurity from 0.15 to 0.5 μm is almost uniform.

Diffusion of halide elements in silicon is rapid at elevated temperatures. Even a high dose of BF $_2$ shows almost no F remaining after a 700 °C anneal.⁴⁵ The results for F, Cl, Br, and I in SiO $_2$ indicate that impurity movement starts at

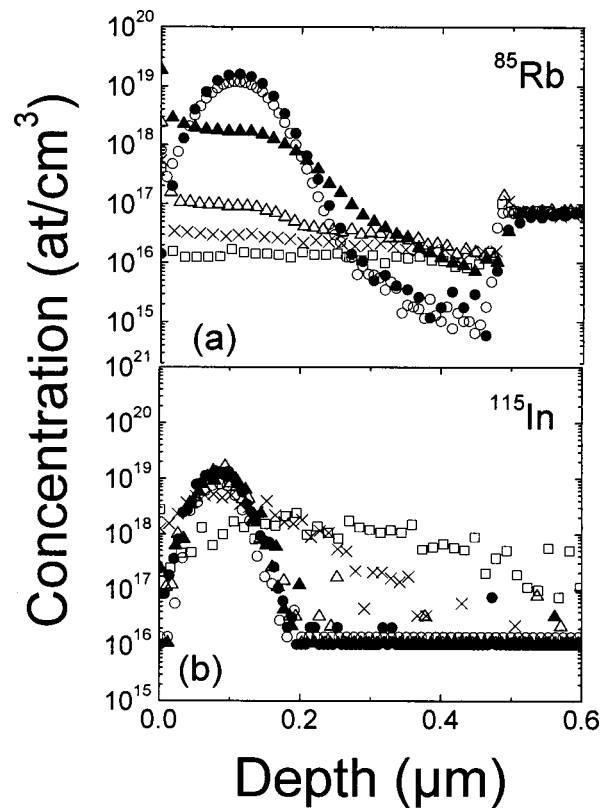


FIG. 5. SIMS depth profiles of: (a) ^{85}Rb (180 keV, $7.5E13$ atoms/cm 2), (b) ^{115}In (150 keV, $9.2E13$ atoms/cm 2): (●) as implanted, (○) 300 °C, (▲) 500 °C, (△) 700 °C, (×) 900 °C, (□) 1000 °C.

700 °C (see Figs. 6 and 7). By 900 °C, all of the halide atoms have diffused out of the oxide and are not detected in a SIMS depth profile. It is notable that this pattern of diffusion holds true for elements as different in mass as F and I.

Of particular interest are the results showing no diffusion of Ga in SiO $_2$ [Fig. 3(b)]. Gallium is the source used in focused ion beam (FIB) systems for sputtering of materials at high lateral resolution. The gallium diffusion data are important because they support the concept of analysis of a patterned silicon wafer using FIB and then reinsertion of the wafer back into the manufacturing process. A significant concern has been the contamination of the process instrumentation, such as gate oxide deposition or diffusion furnaces, by the gallium from the FIB. Another study⁴¹ has also shown the lack of diffusion of Ga in SiO $_2$.

IV. SUMMARY

Analyses of implanted species annealed in thermally grown SiO $_2$ show significantly less diffusion than that seen for the same species in silicon. The results are important to determine which contaminants are mobile and presumably more threatening to the performance of a semiconductor structure. Note that most anneals after oxide deposition in silicon technology are less than 500 °C, and hence the lack of movement of most species examined here can be viewed as a positive result if these elements are under consideration for introduction into the integrated circuit manufacturing process. Similarly, Ga ions, frequently used in chip process-

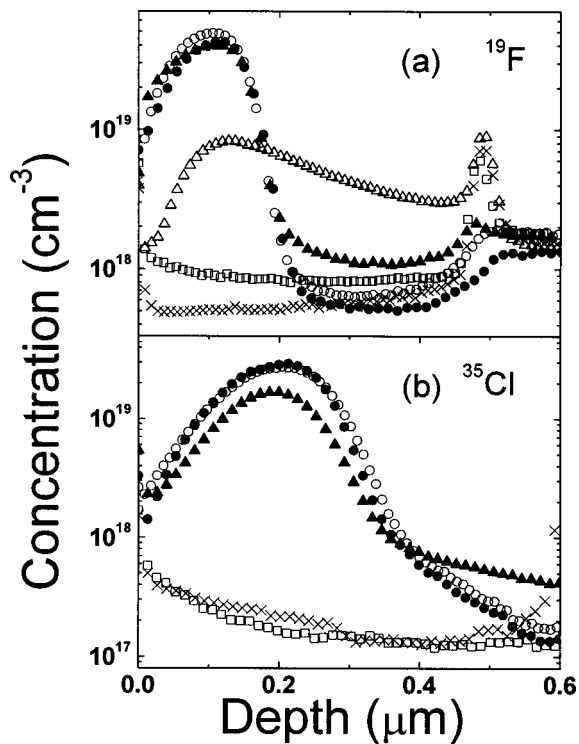


FIG. 6. SIMS depth profiles of: (a) ^{19}F (50 keV, $5E14$ atoms/cm 2), (b) ^{35}Cl (150 keV, $5E14$ atoms/cm 2): (●) as implanted, (○) 300 °C, (▲) 500 °C, (△) 700 °C, (×) 900 °C, (□) 1000 °C.

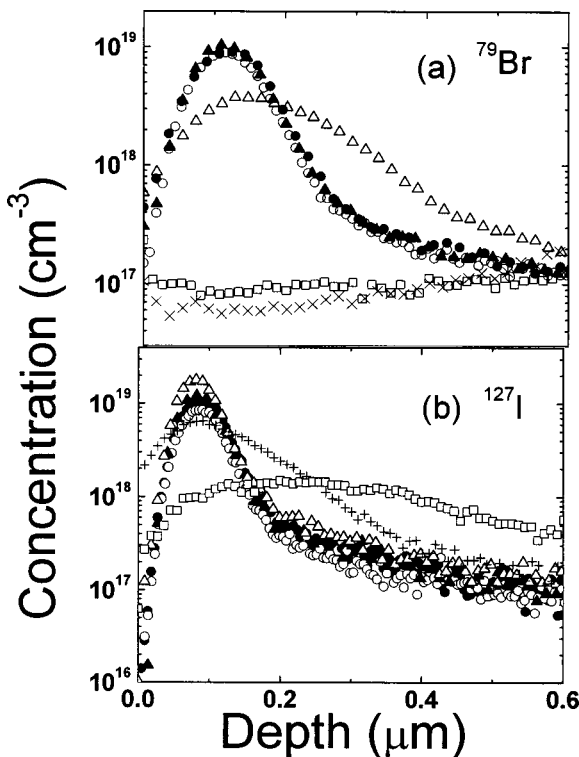


FIG. 7. SIMS depth profiles of: (a) ^{79}Br (180 keV, $1.2E14$ atoms/cm 2), (b) ^{127}I (180 keV, $8.8E13$ atoms/cm 2): (●) as implanted, (○) 300 °C, (▲) 500 °C, (△) 700 °C, (×) 900 °C, (□) 1000 °C.

ing repairs and sample preparation made using a FIB instrument, exhibited minimum diffusion with anneal. It is intended to expand this study to bulk SiO_2 and to determine the effect of the addition of other components to SiO_2 .

ACKNOWLEDGMENTS

The authors acknowledge technical support from the Materials Characterization Facility at University of Central Florida. L.C. would like to acknowledge Fatma Salman of University of Central Florida for assistance in plotting the figures.

- ¹R. N. Hall and J. H. Racette, *J. Appl. Phys.* **35**, 379 (1964).
- ²D. L. Kendall and D. B. DeVries, *Diffusion in Silicon*, Semiconductor Silicon, edited by R. R. Habereck and E. L. Kern (Electrochemical Society Inc., New York, 1969), p. 414.
- ³P. M. Fahey, P. B. Griffin, and J. D. Plummer, *Rev. Mod. Phys.* **61**, 289 (1989).
- ⁴W. E. Beadle, J. C. C. Tsai, and R. D. Plummer, *Quick Reference Manual for Silicon Integrated Circuit Technology* (Wiley, New York, 1985), pp. 6-33-6-35.
- ⁵*Diffusion in Silicon: 10 Years of Research*, edited by D. J. Fisher (Trans Tech Publications, 1999).
- ⁶R. B. Fair, in *Semiconductor Materials Processing Technology Handbook*, edited by G. E. McGuire (Noyes, Park Ridge, N.J., 1988).
- ⁷*Defect and Diffusion in Ceramics: An annual Retrospective I*, edited by D. J. Fisher (Trans Tech, 1999).
- ⁸M. Ghezzi and D. M. Brown, *J. Electrochem. Soc.* **120**, 146 (1973).
- ⁹A. Atkinson, in *Encyclopedia of Materials Science and Engineering*, edited by M. Bever (Pergamon, Oxford, 1986), Vol. 2, p. 1175.
- ¹⁰N. P. Bansal and R. H. Doremus, *Handbook of Glass Properties* (Academic, Orlando, FL, 1986).
- ¹¹M. A. Lamkin, F. L. Riley, and R. J. Fordham, *J. Eur. Ceram. Soc.* **10**, 347 (1992).
- ¹²J. D. McBrayer, R. M. Swanson, and T. W. Sigmon, *J. Electrochem. Soc.* **133**, 1242 (1986).
- ¹³R. H. Doremus, *Phys. Chem. Glasses* **10**, 28 (1969).
- ¹⁴E. Yon, W. H. Ko, and A. B. Kuper, *IEEE Trans. Electron Devices* **13**, 276 (1966).
- ¹⁵R. N. Ghoshtagore, *J. Appl. Phys.* **40**, 4374 (1969).
- ¹⁶Y. Shacham-Diamand, A. Dedhia, D. Hoffstetter, and W. G. Oldham, *J. Electrochem. Soc.* **140**, 2427 (1993).
- ¹⁷J. D. McBrayer, R. M. Swanson, and J. Bravman, *Appl. Phys. Lett.* **43**, 653 (1983).
- ¹⁸D. R. Collins, D. K. Schroder, and C. T. Sah, *Appl. Phys. Lett.* **8**, 323 (1966).
- ¹⁹C. W. Magee and W. L. Harrington, *Appl. Phys. Lett.* **33**, 193 (1978).
- ²⁰T. Yamaji and F. Ichikawa, *J. Appl. Phys.* **59**, 1981 (1986).
- ²¹T. Yamaji and F. Ichikawa, *J. Appl. Phys.* **64**, 2365 (1988).
- ²²T. C. Nason, G. R. Yang, K. H. Park, and T. M. Lu, *J. Appl. Phys.* **70**, 1392 (1991).
- ²³B. Yu, N. Konuma, and E. Arai, *J. Appl. Phys.* **70**, 2408 (1991).
- ²⁴C. L. Schutte and G. M. Whitesides, *Chem. Mater.* **2**, 576 (1990).
- ²⁵I. Mizushima *et al.*, *Jpn. J. Appl. Phys., Part 1* **36**, 1165 (1997).
- ²⁶D. A. Ramappa, Ph.D. dissertation, University of South Florida, FL, 1999.
- ²⁷G. Brebec, R. Seguin, C. Sella, J. Bevenot, and J. C. Martin, *Acta Metall.* **28**, 327 (1980).
- ²⁸H. A. Schaeffer, *J. Non-Cryst. Solids* **38/39**, 545 (1980).
- ²⁹R. Pfeffer and M. Ohring, *J. Appl. Phys.* **52**, 777 (1981).
- ³⁰G. Roma, Y. Limoge, and S. Baroni, *Phys. Rev. Lett.* **86**, 4564 (2001).
- ³¹J. C. Mikkelsen, Jr., *Appl. Phys. Lett.* **45**, 1187 (1984).
- ³²R. Kelly and L. Q. Nghi, *Proceedings of International Conference on Ion Implantation in Semiconductors*, edited by F. H. Eisen and L. T. Chadder-ton, 1971, p. 215.
- ³³H. Francois-Saint-Cyr, E. Anoshkina, F. Stevie, L. Chow, K. Richardson, and D. Zhou, *J. Vac. Sci. Technol. B* **19**, 1769 (2001).
- ³⁴A. H. van Ommen, *J. Appl. Phys.* **56**, 2708 (1984).
- ³⁵A. H. van Ommen, *J. Appl. Phys.* **57**, 1872 (1985).
- ³⁶A. H. van Ommen, *J. Appl. Phys.* **57**, 5220 (1985).
- ³⁷A. H. van Ommen, *J. Appl. Phys.* **61**, 993 (1987).
- ³⁸A. H. van Ommen, *Appl. Surf. Sci.* **30**, 244 (1987).

- ³⁹H. L. Hughes, R. D. Baxter, and B. Phillips, *IEEE Trans. Nucl. Sci.* **NS-19**, 256 (1972).
- ⁴⁰C. W. Magee and W. L. Harrington, *Appl. Phys. Lett.* **33**, 193 (1978).
- ⁴¹R. Welland *et al.*, *Proceedings 26th International Symposium for Testing and Failure Analysis*, Bellevue, WA, November 2000, p. 393.
- ⁴²G. Y. Wong and F. S. Lai, *Appl. Phys. Lett.* **48**, 1658 (1986).
- ⁴³A. La Ferla, G. Galvagno, S. Rinaudo, V. Raineri, G. Franco, M. Camal-
leri, A. Gasparotto, A. Carnera, and E. Rimini, *Nucl. Instrum. Methods Phys. Res. B* **116**, 378 (1996).
- ⁴⁴P. Zhang, MS thesis, University of Central Florida, FL, 2001.
- ⁴⁵M. Y. Tsai, B. G. Streetman, P. Williams, and C. A. Evans, Jr., *Appl. Phys. Lett.* **32**, 144 (1978).
- ⁴⁶T. Takahashi, S. Fukatsu, and K. M. Itoh, *J. Appl. Phys.* **93**, 3674 (2003).
- ⁴⁷J. C. Mikkelsen, *Appl. Phys. Lett.* **45**, 1187 (1984).